

# Mode-resolved transmission functions: an individual Caroli formula

**Hocine Boumrar, Hand Zenia, and Mahdi Hamidi**

Laboratoire de Physique et Chimie Quantique (LPCQ), Université  
Mouloud Mammeri, 15000 Tizi-ouzou, Algeria

E-mail: hand.zenia@ummo.dz

**Abstract.** Efficient manipulation of energy at the nanoscale is crucial for advancements in modern computing, energy harvesting, and thermal management. Specifically, controlling quasiparticle currents is critical to these ongoing technological revolutions. This work introduces a novel and physically consistent approach for computing polarization-resolved transmission functions, a crucial element in understanding and controlling energy transport across interfaces. We show that this new method, unlike several previously derived formulations, consistently yields physically meaningful results by addressing the origin of unphysical behavior in other methods. We demonstrate that while multiple decompositions of the transmission function are possible, only there is a unique and unambiguous route to obtaining physically meaningful results. We highlight and critique the arbitrary nature of these alternative decompositions and their associated failures. While developed within the framework of phonon transport, the individual Caroli formula is general and applicable to other fermionic and bosonic quasiparticles, including electrons, and to internal degrees of freedom such as spin and orbital polarization. Through a comparative analysis using a simple model system, we validate the accuracy and reliability of the individual Caroli formula in capturing polarization-specific transmission properties. This new method provides a more accurate understanding of both phonon and electron transport, offering novel ways for optimization of thermoelectric devices and energy-efficient computing technologies.

## 1. Introduction

Advances in information technology require miniaturization to keep up with the demand for higher performance. One of the challenges, however, is efficient dissipation of the increased heat produced as the result of scaling down the electronic components. Conversely, in applications of thermoelectricity it is the lack of such efficient dissipation (or impedance) that is sought after. Indeed a strongly suppressed thermal conductance is crucial to keep a temperature gradient across a thermoelectric conversion “device”, necessary for its operation[9]. However, the need for both high electrical conductivity and low thermal conductivity is hard to achieve in conventional materials. A thorough understanding of how phonons are transmitted across interfaces is paramount for the design and optimisation of nanoscale devices.

The problem of thermal transport can be treated at different lengthscales. On the largest scale the acoustic mismatch model (AMM) and the diffuse mismatch model(DMM) rely on “an idealized model of the phonon dispersion” and “ignore the contribution from optical phonon modes”[18, 25]. At a “smaller lengthscales” the Boltzmann transport equation (BTE) is used[19]. Here two methods are distinguished: gray and nongray. In the nongray phonon BTE detailed information about dispersion and polarization of the phonon modes is required to accurately capture the physics of phonon transport[27]. This information can only be obtained by considering the lowest scale of all. This is the “mesoscopic/nanoscale” scale where the phonon mean free path is larger than the “device” and ballistic transport is dominant. At this scale one obtains extra information on the phonon dispersion and polarization as well as on the dependence of the

transmittance and reflexion on them. One such piece of information is the contribution of the optic modes to the phonon transport which is completely ignored at larger lengthscales. The other regards mode-resolved or polarization-resolved transmittance. The equivalent quantity in optics is the change of the polarization of light when it passes through a medium. As in optics, we usually (or experimentalists, users) are not interested in the details or mechanisms at play in the scattering region. We would like to know what happens when a phonon (electron) travelling in a single bulk mode (Bloch orbital) of one lead is scattered into the modes (orbitals) that are available in the other lead.

We expect that being able to extract detailed information concerning the transmission function can have further applications such as in nanoelectromechanical systems where proteins can not only be identified by their mass, through shifts in vibration frequency of the modes of the “device” or sensor[24], but also by their configuration through the effect on the polarization-resolved transmission or reflection of the modes.

One can also rely on Molecular Dynamics (MD) to compute phonon transmission by analyzing the energy flux across an interface or through a structure[26]. MD simulations can naturally incorporate unharmonicity and work at high temperatures where classical behaviours dominate[7]. The simulations can fully include both elastic and inelastic scattering events, as well as the influence of disorders in the structure[17]. However, while MD can calculate mode-dependent transmission, it is challenging to extract detailed, mode-resolved reciprocal-space information from real-space data[16][20].

Landauer was the first to find/publish a phenomenological expression for conductance in a two-terminal setup in terms of transmission probabilities[14, 15]. Caroli later on put the formalism on a firm footing by providing a formula to compute the transmission function given a model system (in the harmonic approximation for phonons and in the tight-binding approximation for the electrons)[5]. The necessary parameters (force constants for phonons and site energies and hopping and overlap integrals for the electrons) for the model can nowadays be obtained directly from first-principles calculations[13]. At this stage the required transmission function is obtained using two distinct formalisms: WFM (Wave Function Matching Method)[2, 3, 8, 12] and AGF (Atomistic Green’s Function)[3, 22, 28]. While the two yield identical results, it was not clear how they are related. Recently, however, a rigorous and complete equivalence of the two methods has been shown[3]. In [3] a method of computing polarization-resolved transmission functions was also given.

Before delving into the details concerning computation of mode-resolved phonon or orbital-resolved electron transmission, we feel it is necessary to mention the existence of an alternative way of looking at detailed information on the transmission function. This is known as the eigenchannel decomposition[4]. It is achieved by diagonalising a transmission probability matrix, which is derived from the Green’s functions of the system[13]. The resulting eigenvectors, or eigenchannels, represent the different pathways that phonons can take through the device, with corresponding eigenvalues indicating their transmission probabilities[13]. The focus is put, in this method, on the central part on the subspace of which the scattering states are projected[13]. Hence, the difference with the mode-resolved approach where the focus is rather on the Bloch modes of the leads.

Prior to the method developed in [3] several attempts were made at obtaining mode-resolved transmission functions. The first was by Huang et al.[10] who computed the polarization resolved transmittance by diagonalizing the spectral function which then led to decomposed self-energies. They applied this method to Si/Ge/Si heterogeneous thin film structure. The second attempt was made by Ong and Zhang[21] who based their method on an extension of the AGF formalism. They applied their method to the calculation of mode-resolved transmittance across the graphene–hexagonal boron nitride interface “based on the concept of the Bloch matrix”. They arrived at a similar expression to one published in [3] and later in [11]. The third attempt at obtaining mode-resolved transmittance was developed by Sadasivam et al.[23] and based on the AGF formalism along with the Lipmann-Schwinger equation to obtain surface scattering

states. They applied their method to the Si/Ga interface.

In this work we give a rigorous derivation of the polarization-resolved transmission functions. These, as has already been shown previously in [3] can be obtained from either the formalism of AGF or that of WFM. In [3] the complete equivalence of the two formalisms has already been demonstrated. The advantage of the current derivation is two-fold: (a) the steps involved in the derivation are rigorous and easy to follow, and (b) the amount of time involved in computing the desired quantities is reduced drastically. Our analytical demonstrations and the critique of the earlier methods will be put to the test via a simple model where the comparison is easy to carry out. We use a square lattice and compute the mode-resolved transmission functions using the three methods discussed in this work. The results will be compared to the ones published in [3].

The primary quantity that carries information on the bulk modes and that appears explicitly in the Caroli formula for the transmittance is the escape rate  $\Gamma$ . Indeed, even though  $\Gamma = i(\Sigma - \Sigma^\dagger)$  is written in terms of the surface self-energy  $\Sigma$ , the latter appears only implicitly, through the device Green's function  $G_C$ , in the Caroli formula. As such, any attempt at resolving the transmittance in terms of the bulk modes must necessarily lead to decomposed escape rates. There are many seemingly correct ways the escape rate can be decomposed. It appears, however, and for reasons that will be exposed later/below that only one such method leads to physically meaningful results. The others, although mathematically sound "in some cases", yield results that are clearly unphysical, such as negative transmission amplitudes, or transmittances that are greater than unity. In the following we start with a survey of earlier methods available in the literature and comment on their shortcomings, some physical and some even mathematical in nature. We then expose our method and argue for its validity and simplicity from the mathematical standpoint. We also make the point why it leads to physically sound and meaningful results. In order to further illustrate the discussion and comparison of the different methods, we consider the simplest case where the merits of each method can be brought out. The goal is to allow for other workers to reproduce our results without the further complications that may arise from using realistic models where the numerics or the parametrisation of the interactions may come in the way of focusing on the main issues at hand.

The paper is organized as follows. In the next section we provide a description of a general setup of a two-terminal device, and an overview of the quantities that are central to understand the derivations put forth by the methods. These will be discussed/reviewed in the third section; where our method is also presented. In the fourth section the methods are applied to a simple model for a numerical calculation of the mode-resolved transmittance functions; where the results are used as a means to validate our comparison of the methods. The main arguments and conclusions are presented in the last section.

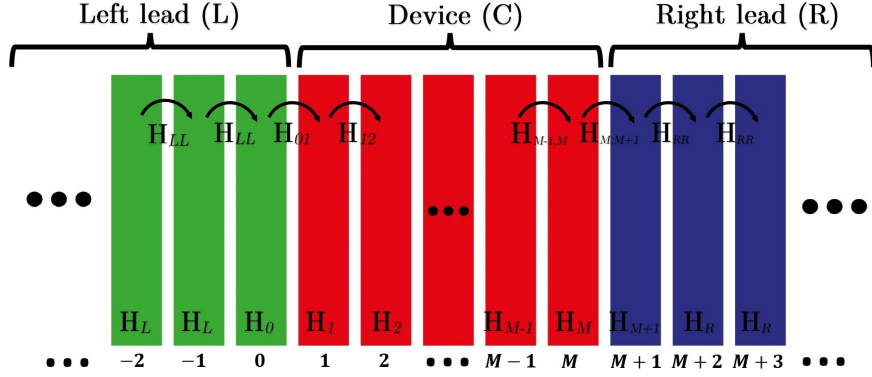


**Figure 1.** Schematic representation of the two-terminal system. It is divided into slices whose corresponding Hamiltonians are also shown.

## 2. The Setup

The total Hamiltonian  $\mathbf{H}$  of the “device”, as shown in Fig. (1), and left and right leads is given by a tridiagonal “supermatrix”:

$$\mathbf{H} = \begin{bmatrix} \ddots & \ddots & 0 & 0 & 0 & 0 & 0 \\ \ddots & \mathbf{H}_L & \mathbf{H}_{LL} & 0 & 0 & 0 & 0 \\ 0 & \mathbf{H}_{LL}^\dagger & \mathbf{H}_L & \mathbf{H}_{LL} & 0 & 0 & 0 \\ 0 & 0 & \mathbf{H}_{LL}^\dagger & \mathbf{H}_C & \mathbf{H}_{RR} & 0 & 0 \\ 0 & 0 & 0 & \mathbf{H}_{RR}^\dagger & \mathbf{H}_R & \mathbf{H}_{RR} & 0 \\ 0 & 0 & 0 & 0 & \mathbf{H}_{RR}^\dagger & \mathbf{H}_R & \ddots \\ 0 & 0 & 0 & 0 & 0 & \ddots & \ddots \end{bmatrix}, \quad (1)$$

where  $\mathbf{H}_L$  and  $\mathbf{H}_R$  are, respectively, the Hamiltonian of a single slice in the left and right leads;  $\mathbf{H}_{LL}$  and  $\mathbf{H}_{RR}$  are the “force constants” between two neighboring slices in the left and right leads, respectively; and  $\mathbf{H}_C$  is the Hamiltonian of the central part attached to the leads. Note that each of these quantities are in general  $n \times n$  matrices, where  $n$  is the number of the degrees of freedom and also of the normal modes.

First, the leads are treated as semi-infinite systems and their respective surface GFs  $g_L$  and  $g_R$  are computed, mostly using a well-known algorithm due to Lopez-Sancho[REFS]. Then, the effect of the presence of the leads on the “central region” is accounted for by left and right self-energies defined as

$$\Sigma_L = \mathbf{H}_{LL}^\dagger g_L \mathbf{H}_{LL} \quad (2)$$

and

$$\Sigma_R = \mathbf{H}_{RR} g_R \mathbf{H}_{RR}^\dagger. \quad (3)$$

These are now added to the first and last diagonal elements of  $H_C$  to give  $H_C^{eff}$ . As a result  $H_C^{eff}$  is no longer Hermitian, a sign that the central region is to be treated as an open system. Inversion of  $H_C^{eff}$  then yields  $G_C$ . Two further important quantities are defined

$$\Gamma_{L(R)} = i(\Sigma_{L(R)} - \Sigma_{L(R)}^\dagger), \quad (4)$$

and are called “escape rates”. Given all the quantities, the total transmission function is given by the Caroli formula

$$t = \text{Tr} \left( \Gamma_L \mathbf{G}_C \Gamma_R \mathbf{G}_C^\dagger \right). \quad (5)$$

All the methods discussed below aim at obtaining mode-resolved escape rates  $\Gamma_{L,i}$  and  $\Gamma_{R,i}$ . These are then plugged into the above Caroli formula to obtain mode-resolved transmittance functions:

$$t_{i,j} = \text{Tr} \left( \Gamma_{L,i} \mathbf{G}_C \Gamma_{R,j} \mathbf{G}_C^\dagger \right) \quad (6)$$

### 3. Earlier Derivations

As mentioned earlier, any attempt at obtaining mode-resolved transmittance functions ought to lead to resolved escape rates. In this section we review two methods that have been published in the literature [10, 23], present a method to correct one of these, and elaborate on a third method developed by us to further illustrate the reason behind the failures of the earlier ones, even when the decomposition is seemingly correctly carried out. The first methods begin by decomposing the spectral function[10], the second starts from the decomposition of the surface Green’s functions[23]. Given that the latter is incomplete, we show how to correct it following the original line of reasoning of its authors. We then exposed a third possible method that consists of starting the decomposition from quantities known as the Bloch matrices.

#### 3.1. Method I: Decomposing the Spectral Function

In this method due to Huang et al.[10] the mode-resolved escape rates are obtained simply by diagonalizing the spectral function  $A$  obtained from the surface GFs  $g_L$  and  $g_R$ . It starts with these expressions of the escape rates :

$$\begin{cases} \Gamma_L = \mathbf{H}_{LL}^\dagger \mathbf{A}_L \mathbf{H}_{LL}, \\ \Gamma_R = \mathbf{H}_{RR} \mathbf{A}_R \mathbf{H}_{RR}^\dagger. \end{cases} \quad (7)$$

where  $H_{LL}$  and  $H_{RR}$  are the left and right matrices connecting two adjacent slices of the leads. The matrix  $A_{L(R)}$  left or right spectral function is defined as

$$\mathbf{A}_{L(R)} = i(\mathbf{g}_{l(r)} - \mathbf{g}_{l(r)}^\dagger), \quad (8)$$

with  $\mathbf{g}_{l(r)}$  being the left and right surface Green’s functions. The spectral function is then diagonalized

$$\mathbf{A} = \sum_{i=1}^n \lambda_i \phi_i \phi_i^\dagger, \quad (9)$$

where  $\phi$  and  $\lambda$  are eigenvectors and eigenvalues and  $n$  is the number of normal modes. This “decomposed” matrix is plugged into the above equation, from which the individual escape rates are obtained :

$$\begin{cases} \Gamma_{L,i} = \mathbf{H}_{LL}^\dagger \lambda_{\mathbf{L},i} \phi_{\mathbf{L},i} \phi_{\mathbf{L},i}^\dagger \mathbf{H}_{LL}, \\ \Gamma_{R,i} = \mathbf{H}_{RR} \lambda_{\mathbf{R},i} \phi_{\mathbf{R},i} \phi_{\mathbf{R},i}^\dagger \mathbf{H}_{RR}^\dagger. \end{cases} \quad (10)$$

where  $\Gamma_{L,i}$  and  $\Gamma_{R,i}$  are the individual escape rates that correspond to the left and right leads. These quantities are subsequently plugged into the Caroli formula (Eq. 6) to obtain the mode-resolved transmittance  $t_{i,j}$  between mode  $i$  on the left and mode  $j$  on the right.

At this point, it is important to point out that apparently there is no connection between the eigenvalue  $\lambda_i$  obtained here and the  $i^{\text{th}}$  mode in the lead. The quantities  $t_{i,j}$  therefore cannot represent mode-resolved transmittance between mode  $i$  on the left and mode  $j$  on the right as claimed in [10].

### 3.2. Method II: Decomposing the Surface Green's Functions

**3.2.1. Original Formulation** The method developed by Sadasivam *et al.*[23] begins by decomposing the surface Green's functions into mode-resolved ones starting from "surface modes"  $\psi_L$  and  $\psi_R$ . These are obtained from the original bulk modes  $\phi_{L/R}$  using the Lippmann-Schwinger equation. They use a different method to compute the surface Green's function: a perturbative approach of the Dyson equation, where the unperturbed Hamiltonian  $H_0$  is that of the perfect lead, taken as an infinite bulk; and the perturbation  $V$  is such that it breaks/suppresses interactions between the  $n^{\text{th}}$  and  $n+1^{\text{st}}$  layer of the bulk, where then they become surface layers. This means that  $V_{n,n+1} = -H_{LL}$  for the left lead and  $V_{n,n+1} = -H_{RR}$  for the right lead, with all other  $V_{kl}$  terms vanishing. The surface is represented by the  $n^{\text{th}}$  layer for the left lead, and by the  $n+1^{\text{st}}$  layer for the right lead. In both cases the perturbation is non-zero only between the layers  $n$  and  $n+1$ . Through the Lippmann-Schwinger equation, they obtain the surface "modes" for the left lead as

$$\psi_L = \phi_n - g_L H_{LL} \phi_{n+1},$$

and for the right lead as

$$\psi_R = \phi_{n+1} - g_R H_{RR}^\dagger \phi_n.$$

The surface Green's functions are decomposed as

$$\begin{cases} g_{L,i}(\omega; k_y) = -\frac{ia}{2} \frac{\psi_{L,i} \psi_{L,i}^\dagger}{2\omega v_{L,i}} \\ g_{R,j}(\omega; k_y) = \frac{ia}{2} \frac{\psi_{R,j} \psi_{R,j}^\dagger}{2\omega v_{R,j}} \end{cases} \quad (11)$$

where the indices  $i$  and  $j$  enumerate the normal modes in the left and right leads, respectively, and  $v_{L/R}$  are generalized group velocities[1, 6]. These decomposed surface GFs are to obtain decomposed self-energies as in eqs. 2 and 3, from which the decomposed escape rates are deduced (eq. 4). Then eq. 6 is used to compute the polarization-resolved transmittance. Again, once these quantities are plugged into the Caroli formula as in Eq. 6 to obtain  $t_{i,j}$  the mode-resolved transmittance between mode  $i$  on the left and mode  $j$  on the right.

The claim here is that since only propagating eigenvectors enter the definition of the surface modes, only the corresponding propagating bulk modes contribute to the transmittance. This is questionable since the surface GFs, and the bulk ones incidentally, that enter in  $\psi_{L/R}$  must contain information on both propagating and evanescent modes. Moreover, the surface  $\psi_{L/R}$  is in fact a mixture of bulk modes, and as such there is no one-to-one correspondence between surface and bulk modes.

We carried out numerical calculations using the mode-resolved surface GFs as given in Sadasivam; and we obtained completely incorrect results for the mode-resolved transmission function  $t_{i,j}$ . Even the total transmission, when computed as the sum of the mode-resolved ones, turned out to be incorrect. Our explanation is that the "total", and correctly computed, surface GF  $g_L$  is not identical to the sum of the mode-resolved functions  $g_{L/R,i}$  as given in eq. 11. For this reason the method as originally formulated in [23] has not been used in the numerical application below. Instead, we obtained a corrected formulation along the lines of ref. [23] for the comparison. The corrected formula is discussed next.

**3.2.2. Corrected Formulation** We have pointed earlier that the formulation put forth in ref. [23] was flawed and here we provide our correction. Indeed, we obtained, in the spirit of Sadasivam *et al.*'s work[23], the correct formula for the mode-resolved surface GFs. Using their notation, and Dyson's equation, the surface Green's function can be written as

$$g_L = G_{n,n} - g_L H_{LL} G_{n+1,n},$$

with

$$G_{n+1,n} = B_R G_{n,n},$$

where, obviously, the last quantities are defined for the perfect leads. Here  $B_{L/R}$  are the Bloch matrices defined in eq. 13. Given, on the other hand, that the unperturbed “surface” Green’s function can be written, in terms of the bulk modes, as

$$G_{n,n} = -i \sum_i \frac{\varphi_{L,i} (\varphi_{L,i}^a)^\dagger}{v_{L,i}},$$

where the index  $i$  enumerates the bulk modes and  $v_{L,i}$  is the corresponding “generalized” group velocity, we arrive at

$$g_L = [I - g_L H_{LL} B_L] G_{n,n} = -i \sum_i [I - g_L H_{LL} B_L] \frac{\varphi_{L,i} (\varphi_{L,i}^a)^\dagger}{v_{L,i}} = \sum_i g_{L,i}. \quad (12)$$

Thus, we obtain, from identification,

$$g_{L,i} = -i [I - g_L H_{LL} B_L] \varphi_{L,i} \frac{(\varphi_{L,i}^a)^\dagger}{v_{L,i}}.$$

While the prefactor on the right-hand side is identical to Sadasivam et al’s[23]  $\psi_n$ , the fraction differs from their  $\psi_n^*$ . The other important difference is the extra 1/2 term in their eq. 14. Seemingly, using the corrected formula one expects improved, if not correct, results. As we will see in the numerical application below, however, this is not the case, again due to the presence of the surface  $g_{L/R}$  in the mode resolved  $g_{L/R,i}$  itself. Indeed, as mentioned above the surface GF  $g_{L/R}$  mixes the bulk modes and also contains information on the evanescent modes. As a result  $g_{L/R,i}$  does not correspond solely to the  $i^{\text{th}}$  bulk mode alone. One possible route is to start with mode-resolved Bloch matrices to obtain decomposed surface GFs  $g_{L/R}$ . This method is discussed in the next sub-section.

### 3.3. Method III: Decomposing the Bloch matrices

Starting from the Bloch matrices (see Appendix in [3])

$$\begin{aligned} \mathbf{B}_L &= \mathbf{C}_L \Lambda_L \mathbf{C}_L^{-1} \\ \mathbf{B}_R &= \mathbf{C}_R \Lambda_R \mathbf{C}_R^{-1}, \end{aligned} \quad (13)$$

where  $\mathbf{C}_{L(R)}$  and  $\Lambda_{L(R)}$  are the left(L) and right(R) eigenvectors and eigenvalues, we compute the surface GFs using

$$g_L = B_L H_{LL}^{-1}, \quad (14)$$

for the left surface GF, for instance, with a similar expression for the right one. We can decompose the Bloch functions by using individual eigenvectors and eigenvalues, instead of the corresponding matrices

$$\begin{aligned} \mathbf{B}_L &= \sum_i \mathbf{B}_{L,i} = \sum_i \varphi_{L,i} \lambda_{L,i} \varphi_{L,i}^{-1} \\ \mathbf{B}_R &= \sum_i \mathbf{B}_{R,i} = \sum_i \varphi_{R,i} \lambda_{R,i} \varphi_{R,i}^{-1}, \end{aligned} \quad (15)$$

and obtain the mode-resolved GFs.

$$\begin{aligned} g_{L,i} &= \varphi_{L,i} \lambda_{L,i} \varphi_{L,i}^{-1} H_{LL}^{-1}, \\ g_{R,i} &= \varphi_{R,i} \lambda_{R,i} \varphi_{R,i}^{-1} (H_{RR}^\dagger)^{-1} \end{aligned} \quad (16)$$

These expressions are to be compared with those obtained by Sadasivam *et al.*[23]. The individual self-energies are also obtained from the Bloch matrices as

$$\begin{aligned}\Sigma_{L,i} &= \mathbf{H}_{RR} \mathbf{B}_{R,i} \\ \Sigma_{R,i} &= \mathbf{H}_{LL}^\dagger \mathbf{B}_{L,i},\end{aligned}\quad (17)$$

from which the mode-resolved escape rates are calculated as

$$\begin{aligned}\Gamma_{L,i} &= i(\Sigma_{L,i} - \Sigma_{L,i}^\dagger) \\ \Gamma_{R,i} &= i(\Sigma_{R,i} - \Sigma_{R,i}^\dagger).\end{aligned}\quad (18)$$

The final formulae for these are

$$\Gamma_{R,i} = i(H_{R,R} \varphi_{R,i} \lambda_{R,i} \varphi_{R,i}^{-1} - c.c.) \quad (19)$$

When inserted into the Caroli formula, these are expected to yield the mode-resolved transmission functions  $t_{i,j}$  as in Eq. 6. However, as we will see below, this formula is not entirely correct. Our numerical calculations show that the mode-resolved transmission functions obtained from the above formula are plagued with similar problems encountered when using Sadasivam *et al.*'s[23] original formulation. In the next section we treat a different route which consists of obtaining mode-resolved escape rates directly from individual group velocities. It is the main contribution of this work.

#### 4. Method IV: Decomposing the Escape Rates

In this section we proceed to the derivation of the correct method leading to results in agreement with those obtained in earlier literature[3, 21]. As shown above, starting from the decomposition of the Bloch matrices we obtain mode-resolved escape rates that when plugged into the Caroli formula lead to what seem a legitimate polarisation-resolved transmittivities. When implemented numerically, however, the results are unphysical in the same way as seen with the methods Huang *et al.*[10] and of Sadasivam *et al.*[23]. Besides, and as we will see now it turns out that the decomposed escape rates when carried out ‘‘properly’’ contain extra terms that are absent in Eq. 19. It is this key difference does not show up in one dimension or when the system is set up such that it behaves as if it were one-dimensional.

Our method here consists in computing the mode-resolved escape rates starting from group velocities as follows. We begin by writing the escape rates in terms of the group velocities and the generalized eigenvectors as

$$\begin{aligned}\Gamma_L &= (\mathbf{C}_L^{a\dagger})^{-1} \mathbf{V}_L^a (\mathbf{C}_L^a)^{-1} \\ \Gamma_R &= (\mathbf{C}_R^\dagger)^{-1} \mathbf{V}_R (\mathbf{C}_R)^{-1},\end{aligned}$$

as derived in [3]. Given the group velocity matrices are diagonal, we can decompose the escape rates as

$$\begin{aligned}\Gamma_L &= \sum_i \Gamma_{L,i} \\ \Gamma_R &= \sum_i \Gamma_{R,i},\end{aligned}$$

with

$$\begin{aligned}\Gamma_{L,i} &= (\varphi_{L,i}^{a\dagger})^{-1} \mathbf{V}_L^a(i,i) (\varphi_{L,i}^a)^{-1} \\ \Gamma_{R,i} &= (\varphi_{R,i}^\dagger)^{-1} \mathbf{V}_R(i,i) (\varphi_{R,i})^{-1},\end{aligned}$$

where the inverse of an eigenvector is actually its pseudoinverse.

With the expressions derived in[3] for the group velocities,

$$\begin{aligned}v_L^a(i,j) &= i\delta_{i,j} \left[ (\varphi_{L,i}^a)^\dagger H_{LL} \varphi_{L,i}^a \tilde{\lambda}_{L,i}^a - (\varphi_{L,i}^a)^\dagger H_{LL}^\dagger \varphi_{L,i}^a (\tilde{\lambda}_{L,i}^a)^\dagger \right] \\ v_R(i,j) &= i\delta_{i,j} \left[ (\varphi_{R,i})^\dagger H_{RR} \varphi_{R,i} \lambda_{R,i} - (\varphi_{R,i})^\dagger H_{RR}^\dagger \varphi_{R,i} (\lambda_{R,i})^\dagger \right]\end{aligned}$$



we arrive at the polarisation resolved escape rates

$$\begin{aligned}\Gamma_{L,i} &= i \left( \left( \varphi_{L,i}^a \right)^\dagger \right)^{-1} \left[ \left( \varphi_{L,i}^a \right)^\dagger H_{LL} \varphi_{L,i}^a \tilde{\lambda}_{L,i}^a - c.c. \right] \left( \varphi_{L,i}^a \right)^{-1} \\ \Gamma_{R,i} &= i \left( \varphi_{R,i}^\dagger \right)^{-1} \left[ \varphi_{R,i}^\dagger H_{R,R} \varphi_{R,i} \lambda_{R,i} - c.c. \right] \varphi_{R,i}^{-1}\end{aligned}\quad (20)$$

Again as with the previous methods these are plugged into Eq. (6) to obtain mode-resolved transmittances. We note that the previous formula has extra terms when compared to Eq. (19). And it turns out that these are needed to obtain the correct mode-resolved transmission functions. These are computed next in the numerical application and checked against the other methods and the results obtained in [3].

Comparison of eq. 20 and eq. 19 shows that they differ by an extra term of the form  $\varphi_i^{-1} \varphi_i$  where  $\varphi_i^{-1}$  is the pseudo-inverse of  $\varphi_i$ . It turns out that this term is crucial when the eigenvectors  $\varphi_i$  are not mutually orthogonal. This happens when the displacement cannot be resolved into longitudinal and transverse along the direction of the propagation of the ‘‘current’’. We think that this decomposition is the only sensible one because the information needed to describe the phonon current must contain both the displacements and the corresponding group velocity. In the other methods, only partial information about the modes is retained.

## 5. Numerical application

### 5.1. Model

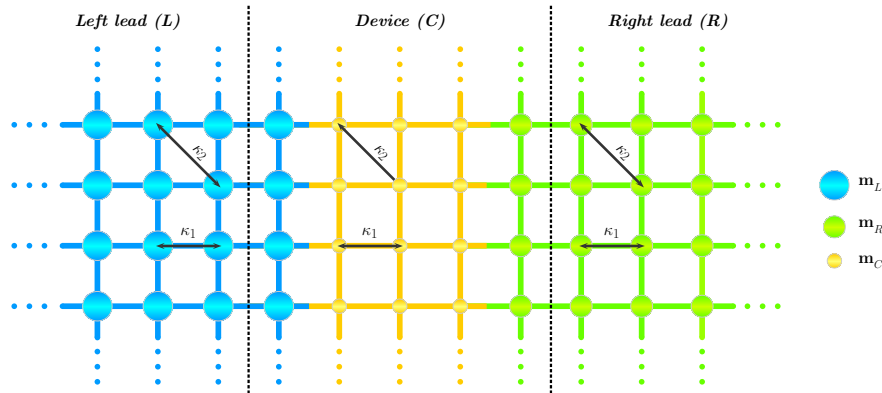


**Figure 2.** A schematic representation the system consisting of a square lattice with the same lattice constant and force constants ( $\kappa_1$  for first-neighbor and  $\kappa_2$  for second-neighbor) throughout. The masses are different in the three regions: they are  $m_L$  in the left lead,  $m_C$  in the central region, and  $m_R$  in the right lead.

In this section we compare different methods of obtaining the desired polarization-resolved transmission functions. Most methods as mentioned earlier rely on resolving one quantity or the other. In some cases it is easy to show when the method fails, but in others we can only rely on numerical simulations to carry out this task. The standard to which all the methods, discussed in this work, are compared is the method published earlier in [3]. As in ref. [3] the merits of each method is gauged by illustrating its application with a simple model, and also by comparing it to previous common methods. We consider the case of the 2D square lattice, of lattice constant  $a$ , with the central part made up of three atomic planes as shown in Fig 2. The force constants are identical throughout the system, but we choose to use a different

mass for each part of the device. The force constants are  $\kappa_1$  and  $\kappa_2 = 0.5 \kappa_1$  for the first and second-neighbor interactions, respectively. The masses are  $m_L$  for the left lead,  $m_R = 0.6 m_L$  for the right lead, and  $m_C = 0.8 m_L$  for the central part. We define the frequency unit  $\omega_0 = \sqrt{\kappa_1/m_L}$ . Henceforth the frequency  $\omega$  is given in units of  $\omega_0$ .

### 5.2. Results

Results of our calculations using the methods outlined in this work are displayed in Figs. 3 and 4 for the transverse wave vectors of  $k_y = 0$  and  $k_y = 1$ , respectively. For  $k_y = 0$  all the methods agree and only one curve is shown. For  $k_y = 1$ , and “possibly” all non-zero  $k_y$ , each method yields a different result. It is easy to see in Fig. 4 that corrected Sadasivam’s method and the method of decomposing the Bloch matrices perform badly, as they yield transmissions that are sometimes negative and sometimes above the maximum of unit transmission. Huang’s method, on the other hand, always gives transmission functions that are positive and less than unity. This seems in the first place that this method is correct. When inspected closely, however, one can see that it gives non-vanishing transmission even when the dispersion curve clearly shows that either of the corresponding modes are evanescent. In light of these remarks, all three mentioned are deemed incorrect when based solely on the numerical results. Our method which consists of starting the decomposition process from the escape rates is the only method that yield correct results when compared to the previously published results.

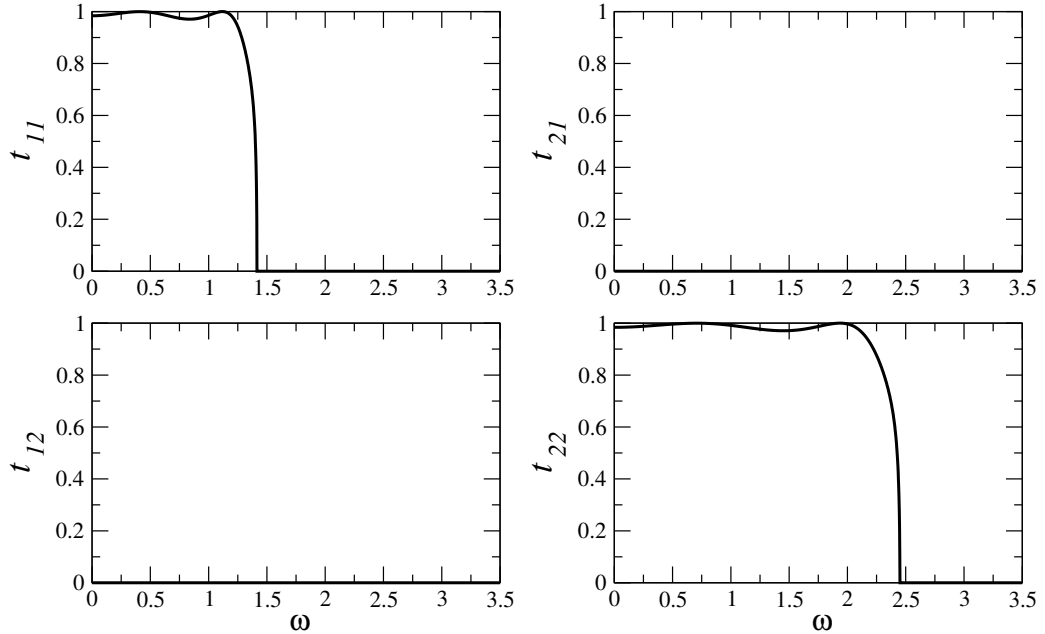


**Figure 3.** Polarization-resolved transmission functions obtained for  $k_y = 0$ .

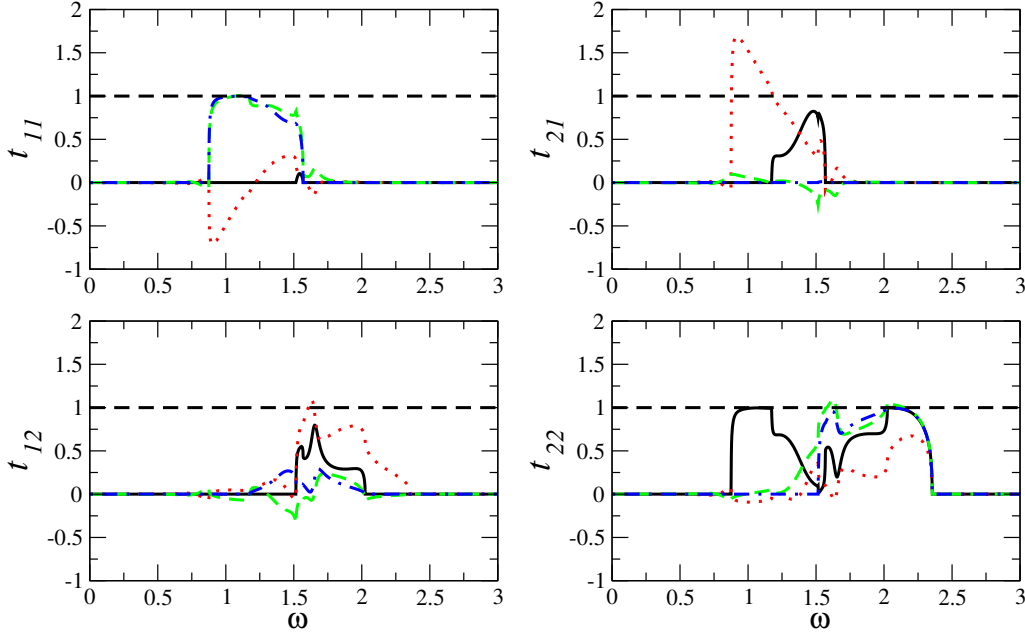


**Figure 4.** Polarization-resolved transmission functions obtained using Huang's method(black continuous), corrected Sadasivam's(red dotted), Bloch matrix decomposition(green dashed), and escape rates decomposition(blue dot-dashed)., for  $k_y = 1$ .

### 5.3. Discussion

It is remarkable that all the methods agree when the transverse momentum  $k_y = 0$ . This can be explained by: (a) the  $u$ 's are orthogonal, and (b) the system is effectively one-dimensional. In the following, therefore, we limit our discussion to the non-vanishing transverse momentum. This case is represented by the value  $k_y = 1$  considered in the current numerical application.

We have seen from the results of the numerical calculations of the mode-resolved transmission functions obtained by Huang *et al.*[10] that they are in disagreement from the ‘‘correct’’ results obtained using our method and the earlier correct ones. We saw that the total transmission is always correct and the mode-resolved functions are also well-behaved, meaning they are always positive and less than or equal unity. These characteristics by themselves do not allow to draw any conclusion as the correctness of the method. The unmistakable flaw of the method, however, is shown when the mode-resolved functions are non-zero (do not vanish) even when either mode is evanescent. This feature does not even call to comparison to other methods, the result being utterly unphysical. Moreover, Huang *et al.*'s method(Method I)[10] yields results that are incorrect when compared to our method, even when both modes are propagating. It is clear that the problem lays in the way the decomposition is carried out within this method. Indeed, and as mentioned above there is no obvious connection between eigenvalues  $\lambda_i$  obtained the  $i^{\text{th}}$  mode in the lead, and as such the resulting  $t_{i,j}$  cannot represent genuine mode-resolved transmission functions.

If we now use this corrected mode-resolved surface GF (Method II), the results are even worse. We obtain for instance negative transmission functions and functions that are greater than unity, even though the total transmission is still correct. The last observation is the difference with the results obtained using the original formulation derived in [23]. This is due to the total surface GF being identical to the sum of the

mode-resolved ones in (Method II); a condition missing in the original formulation of the method.

The apparently better method (Method III) still yields results that in total disagreement with the methods of reference. This method is also plagued with similar incorrect and physically nonsensical results as those obtained from Sadasivam’s method. Again, this tells us that starting from mode-resolved surface GFs is not the right way to proceed. From the last observations we note that even when carried out correctly the resolution of surface GF into individual GFs yields incorrect results. We conclude, therefore, that starting from resolved GFs is not the right way to compute mode-resolved transmission functions

Our method (Method IV) when compared to the earlier method in [3] yields identical results. We assert that the only way to obtain physically correct and meaningful mode-resolved transmission functions is to start from mode-resolved escape rates  $\Gamma_{L/R}$ . These decomposition starts from group velocities, rather than from surface GFs. Using Caroli’s formula

$$t_{\alpha,\beta} = \text{Tr} [\Gamma_{L,\alpha} G_c \Gamma_{R,\beta} G_c^\dagger],$$

it is clear, for instance, that if either mode is evanescent, the resulting transmission vanishes. That this is the case is due to the escape rates being computed directly from the group velocities. This, at least, eliminates the possibility of obtaining non-zero transmission when either mode is evanescent; a problem encountered in both Method I and Method II.

## 6. Conclusion

In this work we have discussed several methods of calculating the polarization-resolved transmittances in the phonon transport problem. Each method carries out the decomposing from a different starting point. The final step in all of them is obtaining mode-resolved escape rates which are then plugged into the Caroli formula to yield mode-resolved transmittances. While some methods are easily shown to be incorrect by analytical means, most seem to be inherently correct. That is until confronted to the genuinely correct methods of decomposition through numerical calculations. Even then, and for a set of given parameters such  $k_y = 0$ , the results may come out correct. This a clear indication that when the tests are also carried out only for a one-dimensional system, the result may give a misleading impression of correctness. It is therefore also fortunate that one can draw unmistakable conclusions from the value of each method by simulating such a simple model as a square lattice. Our aim in choosing this model as mentioned earlier is to make our calculations easy to reproduce, while making our conclusions stand on a firm grounding. It is indeed unfortunate that when a novel method is introduced more often than not the numerical application is carried out on complicated systems with unpublished parameters, rendering reproduction of the results a daunting task to other workers not involved in the work. To conclude, we state that of all the ways of decomposing the transmittance functions, the only correct one is to start from decomposed escape rates which are written directly in terms of “generalized” group velocities.

## References

- [1] Roland E. Allen. Green’s function and generalized phase shift for surface and interface problems. *Phys. Rev. B*, 19:917–924, Jan 1979.
- [2] T. Ando. Quantum point contacts in magnetic fields. *Phys. Rev. B*, 44:8017–8027, Oct 1991.
- [3] Hocine Boumrar, Mahdi Hamidi, Hand Zenia, and Samir Lounis. Equivalence of wave function matching and green’s functions methods for quantum transport: generalized fisher–lee relation. *Journal of Physics: Condensed Matter*, 32(35):355302, 2020.

- [4] M. Büttiker. Coherent and sequential tunneling in series barriers. *IBM Journal of Research and Development*, 32(1):63–75, 1988.
- [5] C Caroli, R Combescot, D Lederer, P Nozieres, and D Saint-James. A direct calculation of the tunnelling current. ii. free electron description. *Journal of Physics C: Solid State Physics*, 4(16):2598, nov 1971.
- [6] Yia-Chung Chang and J. N. Schulman. Complex band structures of crystalline solids: An eigenvalue method. *Phys. Rev. B*, 25:3975–3986, Mar 1982.
- [7] Xiaobin Chen, Yizhou Liu, and Wenhui Duan. Thermal engineering in low-dimensional quantum devices: A tutorial review of nonequilibrium green’s function methods. *Small Methods*, 2(6):1700343, 2018.
- [8] Xiaobin Chen, Yong Xu, Jian Wang, and Hong Guo. Valley filtering effect of phonons in graphene with a grain boundary. *Phys. Rev. B*, 99:064302, Feb 2019.
- [9] Zhang Gang. *Energy Transport and Harvesting : A Computational Study*. Taylor and Francis Group, 2015.
- [10] Zhen Huang, Jayathi Y Murthy, and Timothy S Fisher. Modeling of polarization-specific phonon transmission through interfaces. *Journal of heat transfer*, 133(11), 2011.
- [11] Cailong Jin, Jin Lan, Xuean Zhao, and Wenquan Sui. Mode-detailed analysis of transmission based directly on green’s functions. *Eur. Phys. J. B*, 89:187, 2016.
- [12] Petr A. Khomyakov and Geert Brocks. Real-space finite-difference method for conductance calculations. *Phys. Rev. B*, 70:195402, Nov 2004.
- [13] J. C. Klöckner, J. C. Cuevas, and F. Pauly. Transmission eigenchannels for coherent phonon transport. *Phys. Rev. B*, 97:155432, Apr 2018.
- [14] R. Landauer. Spatial variation of currents and fields due to localized scatterers in metallic conduction. *IBM Journal of Research and Development*, 1(3):223–231, 1957.
- [15] Rolf Landauer. Electrical resistance of disordered one-dimensional lattices. *The Philosophical Magazine: A Journal of Theoretical Experimental and Applied Physics*, 21(172):863–867, 1970.
- [16] Chen Li and Zhiting Tian. Phonon transmission across silicon grain boundaries by atomistic green’s function method. *Frontiers in Physics*, 7, 2019.
- [17] Bolin Liao, editor. *Nanoscale Energy Transport*. 2053-2563. IOP Publishing, 2020.
- [18] W. A. Little. The transport of heat between dissimilar solids at low temperature. *Canadian Journal of Physics*, 37:334–349, 1959.
- [19] Jayathi Y. Murthy, Sreekant V. J. Narumanchi, Jose’ A. Pascual-Gutierrez, Tianjiao Wang, Chunjian Ni, and Sanjay R. Mathur. Review of multiscale simulation in submicron heat transfer. *International Journal for Multiscale Computational Engineering*, 3(1):5–32, 2005.
- [20] Zhun-Yong Ong, Georg Schusteritsch, and Chris J. Pickard. Structure-specific mode-resolved phonon coherence and specularly at graphene grain boundaries. *Phys. Rev. B*, 101:195410, May 2020.
- [21] Zhun-Yong Ong and Gang Zhang. Efficient approach for modeling phonon transmission probability in nanoscale interfacial thermal transport. *Phys. Rev. B*, 91:174302, 2015.
- [22] Carlos A. Polanco. Nonequilibrium green’s functions (negf) in vibrational energy transport: a topical review. *Nanoscale and Microscale Thermophysical Engineering*, 25(1):1–24, 2021.
- [23] Sridhar Sadasivam, Umesh V. Waghmare, and Timothy S. Fisher. Phonon-eigenspectrum-based formulation of the atomistic green’s function method. *Phys. Rev. B*, 96:174302, 2017.

- [24] John E. Sader, Michael L. Roukes, Alfredo Gomez, Adam P. Neumann, and Alex Nunn. Data-driven fingerprint nanoelectromechanical mass spectrometry. *Nature Communications*, 15:8800, 2024.
- [25] E. T. Swartz and R. O. Pohl. Thermal boundary resistance. *Rev. Mod. Phys.*, 61:605–668, Jul 1989.
- [26] JS. Wang, J. Wang, and J. LÄE. Quantum thermal transport in nanostructures. *Eur. Phys. J. B* 6, 381:381–404, 2008.
- [27] Saeid Zahiri, Zhan Xu, Yue Hu, Hua Bao, and Yongxing Shen. A semi-lagrangian method to solve the nongray phonon boltzmann transport equation. *International Journal of Heat and Mass Transfer*, 138:267–276, 2019.
- [28] Yu-Jia Zeng, Zhong-Ke Ding, Hui Pan, Ye-Xin Feng, and Ke-Qiu Chen. Nonequilibrium green’s function method for phonon heat transport in quantum system. *Journal of Physics: Condensed Matter*, 34(22):223001, mar 2022.